0 0 0 0 4 2 0 0 9 3 9

Submitted to Advances In Cryogenic Engineering

LBL-3528
Preprint c.1

JOSEPHSON JUNCTION DEVICES

RECEIVED
LAWRENCE
RADIATION LABORATORY

FEB 20 1975

LIBRARY AND
DOCUMENTS SECTION

John Clarke

November, 1974

Prepared for the U. S. Atomic Energy Commission
under Contract W-7405-ENG-48

For Reference

Not to be taken from this room

LAWRENCE BERKELEY LABORATORY
UNIVERSITY OF CALIFORNIA
BERKELEY

LBL-3528
c.1

DISCLAIMER

This document was prepared as an account of work sponsored by the United States Government. While this document is believed to contain correct information, neither the United States Government nor any agency thereof, nor the Regents of the University of California, nor any of their employees, makes any warranty, express or implied, or assumes any legal responsibility for the accuracy, completeness, or usefulness of any information, apparatus, product, or process disclosed, or represents that its use would not infringe privately owned rights. Reference herein to any specific commercial product, process, or service by its trade name, trademark, manufacturer, or otherwise, does not necessarily constitute or imply its endorsement, recommendation, or favoring by the United States Government or any agency thereof, or the Regents of the University of California. The views and opinions of authors expressed herein do not necessarily state or reflect those of the United States Government or any agency thereof or the Regents of the University of California.

0 0 0 0 4 2 0 6 9 9 0

To be published as an invited review article in
Advances in Cryogenic Engineering (Plenum)

LBL-3528

UNIVERSITY OF CALIFORNIA

Lawrence Berkeley Laboratory
Berkeley, California

AEC Contract No. W-7405-eng-48

JOSEPHSON JUNCTION DEVICES

John Clarke

November 1974

0 0 0 0 4 2 0 6 9 9 1

Josephson Junction Devices*†

John Clarke

Department of Physics, University of California,
and
Inorganic Materials Research Division,
Lawrence Berkeley Laboratory,
Berkeley, California 94720

INTRODUCTION

This article briefly reviews the Josephson effects [1], and discusses two of their applications: to the measurement of voltages, magnetic fields, and magnetic field gradients at or below audio frequencies [2]; and to the detection of high-frequency (microwave and far-infrared) electromagnetic radiation [3]. The paper begins with a brief review of superconductivity and the Josephson effects.

SUPERCONDUCTIVITY

At a sufficiently low temperature, typically a few K, certain metals become superconducting: examples are lead, tin, and niobium. The phenomenon of superconductivity was explained by Bardeen, Cooper

---

* This article is based on a paper published in Science 184:1235, 1974.

† Work supported by the U.S.A.E.C.

and Schrieffer. The basis for their theory was the pairing together of some of the free electrons to form Cooper pairs. These pairs carry the resistanceless current or supercurrent in a superconductor. In any superconductor, all pairs are in a single macroscopic quantum state that may be described by a single wave function or order parameter $\Psi(\vec{r},t) = |\Psi(\vec{r},t)| \exp[i\phi(\vec{r},t)]$. $|\Psi|^2$ represents the pair density, and ϕ is the phase of the order parameter. The absolute value of ϕ is not defined, but (in the absence of currents) the relative phase of the pair quantum state is constant throughout the superconductor, which is said to exhibit phase coherence.

The concept of phase coherence is central to our understanding of superconductivity, and it has intriguing and unique consequences. One of them is zero resistance. Another is flux quantization. Consider a closed superconducting ring that encloses a magnetic flux. The phase ϕ of the order parameter then increases uniformly with distance around the ring. The gradient of the phase is proportional to the enclosed flux. In order for $|\Psi| \exp(i\phi)$ to be single-valued at any point, ϕ must change by $2\pi n$, where n is an integer, in going exactly once around the ring. It is this requirement that imposes flux quantization. The total flux, in general consisting of an applied flux and a flux generated by a persistent supercurrent flowing around the ring, must be equal to $n\phi_o$, where $\phi_o = h/2e \approx 2 \times 10^{-15}$ Wb is the flux quantum.

THE DC JOSEPHSON EFFECT

A third consequence of phase coherence was first pointed out by Josephson [1] in 1962. He considered the behavior of the pair wave function at a junction consisting of two superconductors separated by a thin (1 to 2 nm) insulating barrier, as shown in Fig. 1(a). Above the transition temperature of the superconductors, when the metals are normal, the barrier resistance might be several ohms. However, when the metals are superconducting, Josephson predicted that the barrier resistance would vanish. It would then be possible to pass a small supercurrent through the junction without developing a voltage across it. This process is known as the dc Josephson effect.

The effect involves quantum mechanical tunneling. Cooper pairs are able to "tunnel" from one superconductor to the other through the barrier, retaining their phase coherence in the process. In the absence of any applied fields or currents, the phase is constant through the junction. However, if an external current is passed through the junction, there is a phase change $\delta\phi$ across the barrier. The phase change is governed by the external current through the relation [1],

$$I = I_c \sin(\delta\phi). \tag{1}$$

The maximum value of current that can flow as a supercurrent is I_c, the critical current. The value of I_c depends upon the junction parameters and temperature. If the external current exceeds I_c, a voltage appears across the junction.

THE AC JOSEPHSON EFFECT

When there is a voltage across a Josephson junction, the supercurrent still exists but oscillates with time. This phenomenon is the ac Josephson effect. The frequency ν of the oscillation is related in a simple way to the voltage V across the junction by the Josephson voltage-frequency relation

$$\nu = \frac{2eV}{h} = \frac{V}{\phi_o} . \tag{2}$$

As far as is known at present, this relation is exact. The factor relating frequency and voltage is roughly 484 MHz/μV. The oscillating supercurrents persist for voltages of up to at least several mV and frequencies in excess of 10^{12} Hz.

PRACTICAL JOSEPHSON JUNCTIONS

The best characterized Josephson junction is the tunnel junction [Fig. 1(b)]. Nb-NbO_x-Pb junctions [4] in particular are extremely durable and reliable, and can be repeatedly thermally cycled between room temperature and liquid He^4 temperatures without deterioration.

To make a tunnel junction, one sputters or evaporates a strip of superconductor through a mask onto a glass, sapphire, or quartz substrate. An oxide barrier is grown on the strip, either by a controlled electrical discharge in oxygen, or by thermal oxidation, and a second strip of superconductor is evaporated across the first. The junction therefore consists of two superconducting strips separated by an insulating barrier. Leads are attached to the ends of the strips, and the sample

is cooled to 4.2K. At temperatures well below the transition temperatures of the superconductors, the current-voltage (I-V) characteristic of the junction is similar to that shown in Fig. 1(c). As the current is increased from zero, no voltage appears until the current exceeds the critical current I_c. The voltage then jumps to a nonzero value (dashed line). As the current is increased further and then reduced to zero again, the solid curve is traced out. The critical current may vary from less than 1 μA to hundreds of mA. For the device applications to be described, it is essential to have a reversible I-V curve. The hysteresis is removed by shunting the junction with a strip of normal metal whose resistance R is such that the hysteresis parameter $\beta_c = 2\pi R^2 C I_c/\phi_o < 1$, where C is the junction capacitance.

Two further types of junction are important in device applications. Figure 2(a) shows the Anderson-Dayem bridge [5]. The two superconductors are connected by a superconducting bridge of very small cross section. Because the bridge is so tiny, the maximum supercurrent it can sustain is relatively small. This type of structure was successfully exploited by Mercereau and his group [6], and has since been widely used. The other junction type is the point contact [7] of Zimmerman and Silver [Fig. 2(b)], which has been very popular. The junction consists of a sharpened Nb wire pressed against a flat Nb block. In these junctions, there is no true tunneling process. However, the essential features of Josephson behavior--a limited and phase-dependent supercurrent--are exhibited. All these devices are collectively known as weak links. Figure 2(c) shows the idealized I-V characteristic of all the junction types, including a shunted tunnel junction.

CRYOGENICS

Josephson junction devices are usually operated at 4.2K, the boiling point of liquid helium under atmospheric pressure. The junctions are often immersed in the liquid. However, the boiling of the liquid helium sometimes generates excess noise, and for the most sensitive measurements it may be necessary to mount the device inside a can containing helium gas which is surrounded by the liquid. The traditional low-temperature cryostat consists of a double-walled glass Dewar containing liquid helium surrounded by a second Dewar containing liquid nitrogen. This cryostat is somewhat cumbersome and fragile for use in the field, and more compact and robust versions have been developed, made of metal or fiberglass. The fiberglass Dewar is non-magnetic, an important consideration in the measurement of external magnetic fields. The liquid helium is contained in an inner vessel suspended inside a larger evacuated container. A cooled thermal radiation shield between the two vessels reduces the heat load caused by thermal radiation. A typical cryostat can hold one charge of liquid helium for several days, consuming as little as one liter per day.

SQUIDS

The basic detector for low-frequency measurements is the SQUID (Superconducting Quantum Interference Device). The SQUID combines flux quantization and Josephson tunneling. There are two types of SQUID: the dc SQUID and the rf SQUID.

In the dc SQUID [8], two Josephson junctions are mounted on a superconducting ring [Fig. 3(a)]. The I-V characteristic (which must

be non-hysteretic) is similar to that of a single junction. However, if a magnetic field is applied along the axis of the ring, the combined critical current oscillates as the field is increased. The period of the oscillations with respect to the magnetic flux threading the ring is the flux quantum ϕ_o [Fig. 3(b)]. The critical current has a maximum value when the flux applied to the SQUID is $n\phi_o$ (n is an integer), and a minimum value when the flux is $(n + 1/2)\phi_o$. This periodic behavior reflects the macroscopic quantum nature of the SQUID.

Changes in I_c induce changes in the I-V characteristic, as indicated in Fig. 3(c). In a practical application, the junctions are biased at a nonzero voltage, by a constant current I_o, that always exceeds the maximum value of critical current. If the applied field is changed, the voltage across the SQUID oscillates about its mean value with an amplitude of typically 1 μV. These voltage changes are amplified by conventional room-temperature electronics.

The dc SQUID constructed by Clarke, Goubau, and Ketchen [9], is shown in Fig. 4. A 10 mm long Pb film is evaporated around a 3 mm diameter quartz tube, and then a Au shunt is deposited. Two Nb strips are sputtered and thermally oxidized, and a Pb tee whose crossbar overlays these strips is then evaporated to form two shunted Nb-NbO_x-Pb tunnel junctions. The whole structure is coated with an insulating layer, and finally a Pb ground plane is evaporated over the slit in the Pb cylinder and the various metal strips to reduce the inductance to a minimum. Leads are attached to platinum or gold electrodes baked onto the tube prior to the film depositions. Typical parameters for a SQUID at 4.2K are: critical current ~ 5μA; resistance ~ 0.5 Ω; area, A, of

Pb band ~ 7 mm^2; total SQUID inductance ~ 1 nH; critical current modulation depth ($I_c[n\phi_o] - I_c[(n + 1/2)\phi_o]$) ~ 1 μA; and corresponding voltage modulation ~ 1 μV.

The dc SQUID is thus a digital magnetometer with a basic sensitivity $H_o = \phi_o/A \sim 3 \times 10^{-10}$ T. However, the device is not often used in this mode. Instead, it is incorporated into a feedback circuit, the whole system producing a voltage output that is proportional to changes in the applied flux. The principle is illustrated in Fig. 5. An ac flux at 100 kHz of peak-to-peak amplitude $\lesssim \phi_o/2$ is applied to the SQUID, which is biased at a finite voltage by a constant current I_o. The ac voltage that appears across the SQUID excites a superconducting tank circuit tuned at 100 kHz with Q ~ 200. The form of the ac voltage across the SQUID then depends on the value of the dc flux applied to it. If the flux is $n\phi_o/2$, this voltage is a "rectified" version of the applied ac flux, with a frequency of 200 kHz. This signal is greatly attenuated by the tank circuit. On the other hand, if the applied flux is $(n/2 + 1/4)\phi_o$, the signal across the SQUID is at the fundamental frequency, and is amplified by the tank circuit. For intermediate values of flux, there will be a mixture of 100 kHz and 200 kHz signals, of which only the fundamental is amplified by the tank circuit. Thus as the flux applied to the SQUID is steadily increased from $n\phi_o$, the 100 kHz signal across the tank circuit is initially zero, increases to a maximum at $(n + 1/4)\phi_o$, is zero at $(n + 1/2)\phi_o$, reaches a maximum again (but with opposite phase) at $(n + 3/4)\phi_o$, and so on.

The signal across the tank circuit is amplified by conventional electronics (Fig. 5), and detected by a lock-in referenced to the 100 kHz

oscillator. The output from the lock-in is integrated, and this smoothed signal fed back to the modulation coil coupled to the SQUID. A small flux change $\delta\phi$ applied to the SQUID is thus exactly cancelled by the feedback flux, the feedback current being proportional to the applied flux. The frequency response of the closed loop is about 1 kHz.

It is possible to resolve changes in applied flux corresponding to a small fraction of a flux quantum. The SQUID rms noise above 1 Hz is typically $5 \times 10^{-5}\phi_o/\sqrt{Hz}$. The best figure achieved was about $2 \times 10^{-5}\phi_o/\sqrt{Hz}$, corresponding to a magnetic field resolution of about $6 \times 10^{-15}T/\sqrt{Hz}$. The limiting sensitivity appears to be set by thermal noise in the junctions. At frequencies below 1 Hz, the rms noise increases somewhat. However, if the He^4 bath is temperature stabilized, the long term drift is very small, as indicated in Fig. 6. The upper limit to the drift is $8 \times 10^{-5}\ \phi_o/hr$. It is thought that the higher noise and drift observed with an unstabilized bath may be caused by paramagnetic impurities in the quartz tube. Temperature fluctuations induce susceptibility fluctuations that in turn produce a magnetic flux noise in the SQUID.

The rf SQUID was developed by Mercereau and his co-workers [10], and by Zimmerman and his co-workers [11]. It consists of a single Josephson junction mounted on a superconducting ring (Fig. 7). Here again, a steadily increasing magnetic field induces quantum transitions in the SQUID. If the junction is repetitively driven into a voltage-supporting state, there will be an average circulating supercurrent that is periodic in the applied flux, with a period ϕ_o. This current is detected by coupling the SQUID to the inductance of a resonant tank

circuit (Fig. 7). An alternating current at the resonant frequency (typically 30 MHz) generates an alternating voltage across the resonant circuit. The amplitude of this rf voltage depends on the value of the circulating supercurrent in the SQUID and is therefore periodic in the flux applied to the SQUID. The rf voltage is amplified and rectified by conventional electronics. The detected rf signal is also periodic in the flux. The rf SQUID is generally used in a feedback circuit very similar to that in Fig. 5. An additional low frequency (usually 10 - 100 kHz) flux modulation is applied to the rf SQUID, just as in the case of the dc SQUID, and the resultant signal lock-in detected, integrated, and fed back to maintain the null balance of the SQUID.

Various types of rf SQUID have been made and used successfully. The point contact SQUID of Zimmerman, Thiene, and Harding [11] consisted of a hollow niobium cylinder in which a sharpened niobium screw was tapped [Fig. 8(a)]. The rf coil was mounted inside the ring. The same workers also developed the two-hole SQUID shown in Fig. 8(b). A very ingenious extension of this idea is Zimmerman's "fractional turn" SQUID, in which twelve parallel holes are drilled in a Nb cylinder. The inductance of each hole is connected in parallel across a single point-contact, so that the total inductance is rather low. Consequently, the modulation depth of the rf signal in response to a changing flux (proportional to the inverse square root of the SQUID inductance) is large, so that a smaller flux change can be detected with a given preamplifier. In addition, the effective area of the SQUID is large, so that a given flux change corresponds to a very small change in magnetic field. Consequently, the sensitivity of the device is very high, about

$3 \times 10^{-15} \cdot T/\sqrt{Hz}$ (above 1 Hz) with an rf frequency of 30 MHz.

A second popular type of rf SQUID, first used by Mercereau and his colleagues [10], is shown in Fig. 8(c). A band of superconducting material evaporated around a glass, quartz, or sapphire cylinder contains an Anderson-Dayem bridge. The bridge is usually formed by scribing or by a technique involving photolithography and subsequent etching. The magnetic field sensitivity of the device (above 1 Hz) is typically $10^{-13} T/\sqrt{Hz}$ with a 30 MHz rf frequency.

The resolution of an rf SQUID increases as the square root of the rf driving frequency. Several higher frequency SQUIDs have recently been developed, working at frequencies of up to several GHz. With proper design, these systems have demonstrated the expected increase in sensitivity. Gaerttner has operated a SQUID at 440 MHz that had a sensitivity of $7 \times 10^{-6} \phi_o/\sqrt{Hz}$ at frequencies above a few Hz.

At present, the rf SQUID is more widely used than the dc SQUID, probably because it is commercially available in both thin-film and point contact versions. However, with the exception of the twelve-hole-SQUID, the 30 MHz rf SQUIDs are less sensitive than the dc SQUID. For most practical purposes, either type of SQUID has adequate sensitivity at frequencies above 1Hz. Until recently, relatively little attention seems to have been paid to drift and low frequency noise. The dc SQUID described above, even in a helium bath that is not temperature stabilized, appears to have a much better long-term stability than the commonly used rf SQUIDs. It is probable that the long term stability of rf SQUIDs could also be improved by bath stabilization. This problem will undoubtedly be studied extensively in the near future.

FLUX TRANSFORMER

The superconducting flux transformer, shown schematically in Fig. 9(a), is often used in measurements of magnetic field. The transformer is entirely superconducting and consists of a pick-up loop (primary coil) and a secondary coil tightly coupled to a SQUID. The SQUID and secondary are enclosed in a superconducting can that screens the SQUID from fluctuations in the ambient magnetic field. A magnetic field applied to the pick-up loop generates a persistent current, which in turn induces a flux in the SQUID. The sensitivity of the SQUID can be appreciably enhanced by proper transformer design, and resolutions of better than 10^{-15} $T/\sqrt{Hz}$ have been achieved.

An important development of the flux transformer is the magnetic field gradiometer, illustrated in Fig. 9(b). In this configuration, the transformer has two pick-up coils of equal area. They are arranged so that a uniform magnetic field does not induce a supercurrent. If the field has a gradient $\partial H_z/\partial x$, the fields applied to the two coils will differ and the induced supercurrent will be proportional to the difference. The SQUID system thus measures a gradient. The gradiometer can be made in many configurations: gradiometers measuring $\partial H_z/\partial z$ are commonly used, and higher derivatives can also be measured. The first published account of a gradiometer appears to be that of Zimmerman and Frederick, who reported a resolution of 10^{-12} $T/m/\sqrt{Hz}$. Sensitivities as high as 3×10^{-14} $T/m/\sqrt{Hz}$ have subsequently been reported.

The great advantage of the gradiometer is that it discriminates against noise generated a large distance away, which therefore has a small gradient, in favor of a signal generated close by, which has a

relatively large gradient. It is therefore possible to measure relatively weak magnetic signals produced locally in the presence of much larger fluctuating magnetic fields generated by distant sources. For example, gradiometers have been used successfully to take magnetocardiograms in an unshielded environment. These devices have considerable potential in geophysics and magnetic surveying. A modified gradiometer may also be used to measure magnetic susceptibility. The sample is inserted in one loop of a gradiometer and a uniform magnetic field applied to both loops. The supercurrent generated in the gradiometer is then proportional to the susceptibility of the sample. Mercereau and co-workers have used this technique to measure the susceptibility of biochemical samples over a temperature range from 4K to 300K. The high sensitivity of the SQUID enables one to use minute samples, an important consideration for biological samples.

VOLTMETER

The SQUID is often used as a voltmeter. In Fig. 9(c) a resistance R is in series with a superconducting coil coupled to a SQUID. A signal voltage V_s applied to the terminals generates a current $I_S = V_S/R$ that is detected by the superconducting device. These voltmeters have been widely used in solid state physics to measure tiny voltages. The sensitivity is very great, and voltages as low as $10^{-15} V/\sqrt{Hz}$ can be detected routinely. The resolution is often limited by the Johnson noise generated in the series resistance or the source resistance: the Johnson noise in $10^{-8}\ \Omega$ at 1K is about $10^{-15} V/\sqrt{Hz}$. This fact has been utilized by Giffard, Webb, and Wheatley [12] in their noise thermometer.

The terminals marked V_S in Fig. 9(c) are shorted together, so that the circuit consists of a superconducting loop containing a resistance R. The mean square Johnson noise current is proportional to the absolute temperature and is measured by the SQUID in the usual way. Giffard et al. have been able to measure temperatures down to a few mK with this technique.

EFFECT OF MICROWAVES ON JOSEPHSON JUNCTIONS

If microwaves at frequency f are coupled to a Josephson junction, for example, a point contact, the I-V characteristic is modified as shown in Fig. 10. A series of steps is induced, the voltage along each step being constant. The steps appear at voltages

$$|V_n| = nhf/2e, \tag{3}$$

where n is an integer. The range of current over which the voltage remains constant (that is, the step height) oscillates as the microwave power is increased. The detailed theory of the behavior of a junction in a microwave field is complicated. The essential point is that the microwaves at frequency f are mixed in the nonlinear junction with the ac Josephson currents whose frequency ν depends upon the voltage across the junction. Whenever $(\nu \pm nf) = 0$ (Eq. 2), there is a zero-frequency beat, that is manifested as a current step. A simple quantum description of the effect has been given by Josephson. When the junction is biased at a voltage V, the energy difference between Cooper pairs on opposite sides of the barrier is just 2eV. Whenever this energy

difference is exactly nhf, pairs can cross the barrier coherently with the emission or absorption of n microwave photons.

Josephson junctions can be used as detectors of electromagnetic radiation in a number of different ways. Only two will be discussed here, the square law broadband detector, and the heterodyne linear detector.

SQUARE LAW BROADBAND DETECTOR

The use of a Josephson junction as a broadband detector was first investigated by Grimes, Richards, and Shapiro [13]. When microwaves generate constant current steps, at the same time they reduce the magnitude of the critical current. In fact, the critical current is also an oscillatory function of the microwave field. The critical current corresponds to the n = 0 induced step. Suppose one applies broadband radiation (that is, radiation containing a wide range of frequencies) to a junction. The steps on the I-V characteristic will be blurred out, and no discrete steps will be visible. However, the critical current responds to each frequency component of the radiation and will be correspondingly modified. (Equation 3 is satisfied for n = 0 by all values of frequency f.) The critical current does not respond uniformly to all frequencies, the response becoming less sensitive as the frequency increases. For small signal levels

$$\Delta I_c \propto V_s^2/\omega_s^2, \tag{4}$$

where V_s is the voltage induced across the junction by radiation at a frequency ω_s and ΔI_c is the resulting depression in the critical current. The fact that ΔI_c is proportional to V_s^2 implies that the junction is a square law detector and that it responds to the power rather than to the amplitude of the radiation.

In all successful detectors point-contact junctions have been used. It appears that the point contact couples more efficiently to the radiation than other types of junction, although the coupling properties of Anderson-Dayem bridges are now being extensively studied. The point contact is mounted transversely across a wave guide or light pipe (oversized wave guide) so that the electric field of the incoming radiation generates currents through the junction. The wave guide is usually terminated by a movable plunger which is adjusted to maximize the coupling efficiency. Changes in the critical current in response to radiation are detected by a method identical to that used for the dc SQUID [Fig. 3(c)]. A constant current I_o biases the junction at a non-zero voltage. When the critical current changes, the I-V characteristic and hence the voltage across the junction are modified. Since the detector responds to a wide range of frequencies, the bandwidth is often restricted externally to a narrow range about some central frequency (for example, by an interferometer). One sweeps the central frequency to obtain the spectrum of the radiation. It is usual to chop the incoming radiation at a few tens of hertz and to detect the resulting ac signal that appears across the junction.

There is a particular need for better detectors in the far-infrared, at wavelengths around 1 mm. The best broadband Josephson detectors have

NEP's of $10^{-14} - 10^{-13}$ W/$\sqrt{\text{Hz}}$ at 1 mm. The theoretical limit is about 5×10^{-15} W/$\sqrt{\text{Hz}}$ at 1 mm. The achieved NEP's are not quite as good as those of the best broadband semiconducting bolometers. However, the point contact has a very much faster response time than the high sensitivity semiconducting bolometers. It appears, therefore, that the Josephson detector may be the best available for experiments requiring a fast response, for example, in observing pulsars, or in pulsed laboratory experiments.

HETERODYNE DETECTOR

In the heterodyne detector, the signal to be detected is combined (mixed) with the output from a local oscillator in the nonlinear Josephson junction. In the simplest case, the signal frequency, f_S, is close to the local oscillator frequency, f_{LO}. The amplitude of the local oscillator output is much greater than the signal amplitude. Under these conditions, the signal and local oscillator output add in a relatively simple way, as indicated in the phasor diagram of Fig. 11(a). The local oscillator output is represented by the vector of length A_{LO} rotating at an angular frequency $\omega_{LO} = 2\pi f_{LO}$. To this vector is added the signal vector, of length A_S, rotating at a frequency ω_S. Relative to the local oscillator vector, the signal vector rotates at a frequency $\omega_I = |\omega_{LO} - \omega_S|$ (the intermediate frequency), which is much less than either ω_{LO} or ω_S. The resultant vector A therefore rotates with a frequency ω_{LO}, but its amplitude is modulated at a frequency ω_I between the limits $(A_{LO} + A_S)$ and $(A_{LO} - A_S)$.

The mixing process that occurs in the Josephson junction can be

readily understood. In the absence of a signal, the large local oscillator output induces a series of steps in the I-V characteristic, as shown in Fig. 10. When the signal is applied, the effect of the local oscillator on the junction is modulated at a frequency $f_I = |f_{LO} - f_S|$. Consequently, the whole I-V characteristic is modulated at f_I, as shown in Fig. 11(b). A constant current I_o biases the junction at a voltage roughly one half that of the n = 1 step. In the presence of a signal, the voltage across the junction oscillates at a frequency f_I, and with an amplitude that is proportional to the signal amplitude. This voltage is amplified by an IF amplifier and subsequently measured.

The best characterized Josephson heterodyne detector at present is that of Taur, Claassen, and Richards [14]. They used a point-contact device, mounted in the way described for the broadband detector. The local oscillator frequency was 36 GHz. The noise temperature of their mixer was less than 60K, which makes it the best available at 36GHz. The next step is to extend the local oscillator to ~ 300 GHz. If the mixer noise temperature remains low, as it theoretically should, the Josephson heterodyne detector will be the most sensitive of any available by a substantial margin.

SUMMARY

The use of SQUIDs has given us unprecedented resolution in low frequency measurements. Magnetic field sensitivities of better than 10^{-15} T/$\sqrt{\text{Hz}}$ (using a flux transformer), magnetic field gradient sensitivities of better than 10^{-13} T/m/$\sqrt{\text{Hz}}$, and voltage sensitivities as high as 10^{-15} V/$\sqrt{\text{Hz}}$ are now routinely obtainable. These devices are reliable,

relatively simple and inexpensive to use, and have been operated successfully in the field for both geophysical and medical measurements.

The best Josephson broadband far infrared detectors have NEP's approaching 10^{-14} W/$\sqrt{\text{Hz}}$, and are not quite as sensitive as the best semiconductor bolometers. However, the Josephson detector has a much faster response. The heterodyne detector is the best mixer presently available with a 36 GHz pump frequency, and has great promise for use at higher pump frequencies.

ACKNOWLEDGEMENT

The author is pleased to acknowledge many helpful conversations with Professor P. L. Richards on high frequency detectors.

REFERENCES

1. B. D. Josephson, Phys. Letters 1:251 (1962); Adv. Phys. 14:419 (1965).
2. For a more detailed review, see J. Clarke, Proc. IEEE 61:8 (1973); an extensive list of references is given in this paper.
3. For a more detailed review, see P. L. Richards, F. Auracher, and T. Van Duzer, Proc. IEEE 61:36 (1973); an extensive list of references is given in this paper.
4. J. E. Nordman, J. Appl. Phys. 40:2111 (1969); L. O. Mullen and D. B. Sullivan, J. Appl. Phys. 40:2115 (1969); R. Graeffe and T. Wiik, J. Appl. Phys. 42:2146 (1971); J. Schwidtal, J. Appl. Phys. 43:202 (1972); P. Hansma, J. Appl. Phys. 45:1472 (1974).
5. P. W. Anderson and A. H. Dayem, Phys. Rev. Lett. 13:195 (1964).
6. H. A. Notarys, R-H Wang, and J. E. Mercereau, Proc. IEEE 61:79 (1973).
7. J. E. Zimmerman and A. H. Silver, Phys. Rev. 141:367 (1966).
8. R. C. Jaklevic, J. Lambe, A. H. Silver, and J. E. Mercereau, Phys. Rev. Lett. 12:159 (1964).
9. J. Clarke, W. M. Goubau, and M. B. Ketchen, Proc. of Applied Superconductivity Conference, held at Oakbrook, Ill. Sept. 30-Oct. 2, 1974.
10. J. E. Mercereau, Rev. Phys. Appl. 5:13 (1970); M. Nisenoff, Rev. Phys. Appl. 5:21 (1970); H. A. Notarys and J. E. Mercereau, Proc. Int. Conf. Science of Superconductivity (Stanford, Calif., Aug. 26-29, 1969), F. Chilton, Ed., pp. 424-431.
11. J. E. Zimmerman, P. Thiene, and J. T. Harding, J. Appl. Phys. 41:1572 (1970).
12. R. P. Giffard, R. A. Webb, and J. C. Wheatley, J. Low Temp. Phys. 6:533 (1972).
13. C. C. Grimes, P. L. Richards, and Shapiro, Phys. Rev. Lett. 17:431 (1966); J. Appl. Phys. 31:3905 (1968).

0 0 0 0 4 2 0 7 0 0 1

14. Y. Taur, J. H. Claassen, and P. L. Richards, Revue de Physique Appliquée 9:261 (1974).

FIGURE CAPTIONS

Fig. 1(a) Schematic of Josephson junction; (b) practical tunnel junction; (c) current-voltage (I-V) characteristic of tunnel junction.

Fig. 2(a) Anderson-Dayem bridge evaporated on substrate; (b) point contact; (c) idealized I-V characteristic of Anderson-Dayem bridge, point contact, or shunted tunnel junction.

Fig. 3(a) A dc SQUID: two Josephson junctions (X) on a superconducting ring; (b) oscillations in critical current as a function of applied flux; (c) I-V curves for the SQUID for two values of applied flux: when the applied flux changes from $n\phi_o$ to $(n + 1/2)\phi_o$, the voltage across the SQUID changes by δV.

Fig. 4. Cylindrical dc SQUID with two shunted Nb-NbO_x-Pb tunnel junctions.

Fig. 5. Schematic of dc SQUID electronics.

Fig. 6. Drift of dc SQUID over 3 hr period.

Fig. 7. Tank circuit coupled to rf SQUID.

Fig. 8. Types of rf SQUIDs: (a) Single-hole device made from Nb cylinder; (b) double-hole device, made from Nb cylinder; (c) thin film evaporated onto quartz cylinder.

Fig. 9(a) Flux transformer; (b) gradiometer; (c) voltmeter.

Fig. 10. I-V characteristics of point contact irradiated with microwaves at 4 GHz.

Fig. 11. Heterodyne detector: (a) phasor diagram, showing the addition of A_{LO}, which has a frequency ω_{LO}, and A_s, which has a frequency ω_s. If $\omega_{LO} \approx \omega_s$, the resultant vector A is amplitude modulated at a frequency $\omega_I = |\omega_{LO} - \omega_s|$. (b) The solid line shows the effect of the local oscillator on the I-V characteristic. An applied

signal modulates the characteristic between the limits set by the dotted lines; I_o (dashed line) is a constant current bias.

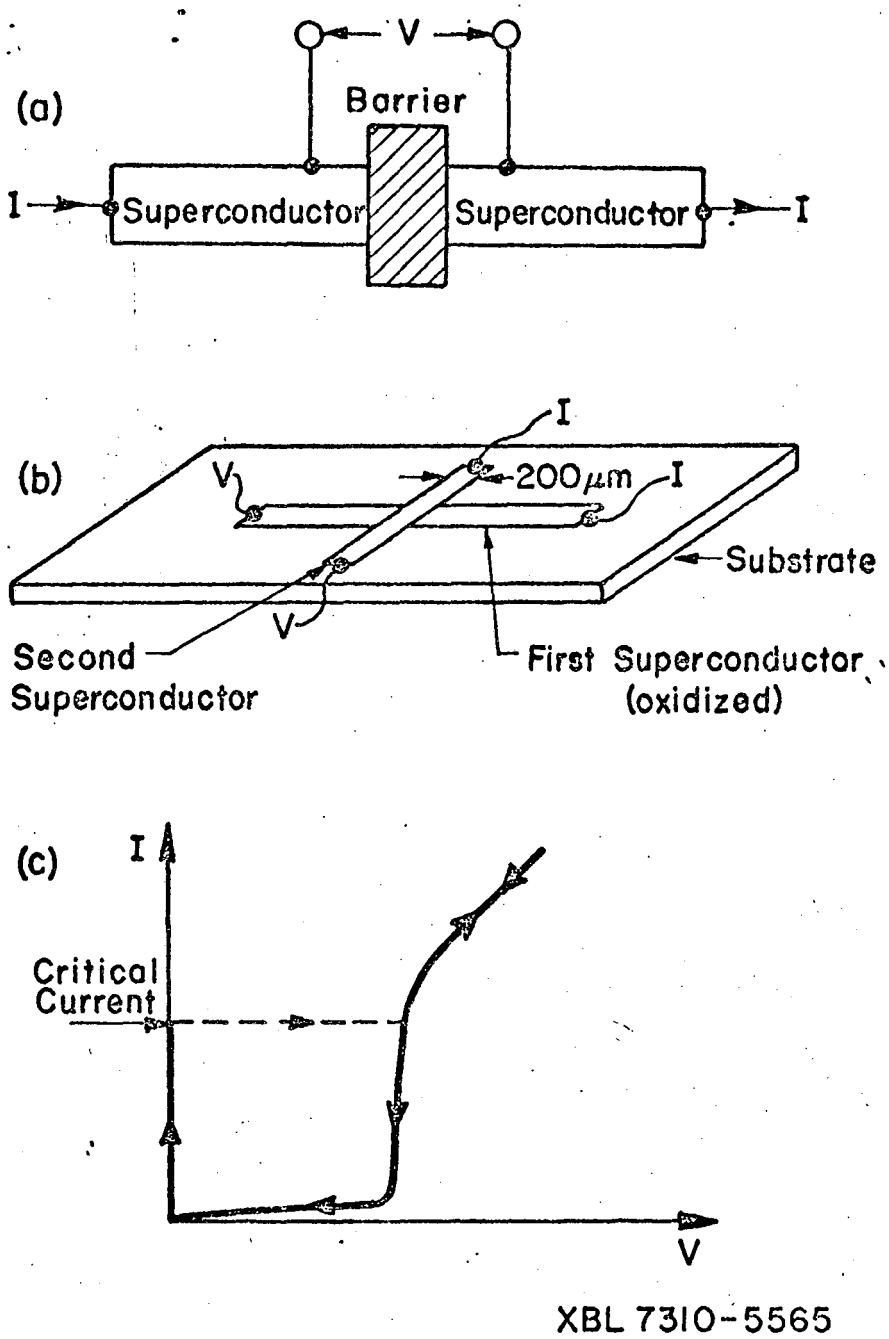
(a)
V
Barrier
I
Superconductor
Superconductor
I
(b)
I
V
200μm
I
Substrate
V
Second
Superconductor
First Superconductor
(oxidized)
(c)
I
Critical
Current
V
XBL 7310-5565

Fig. 1

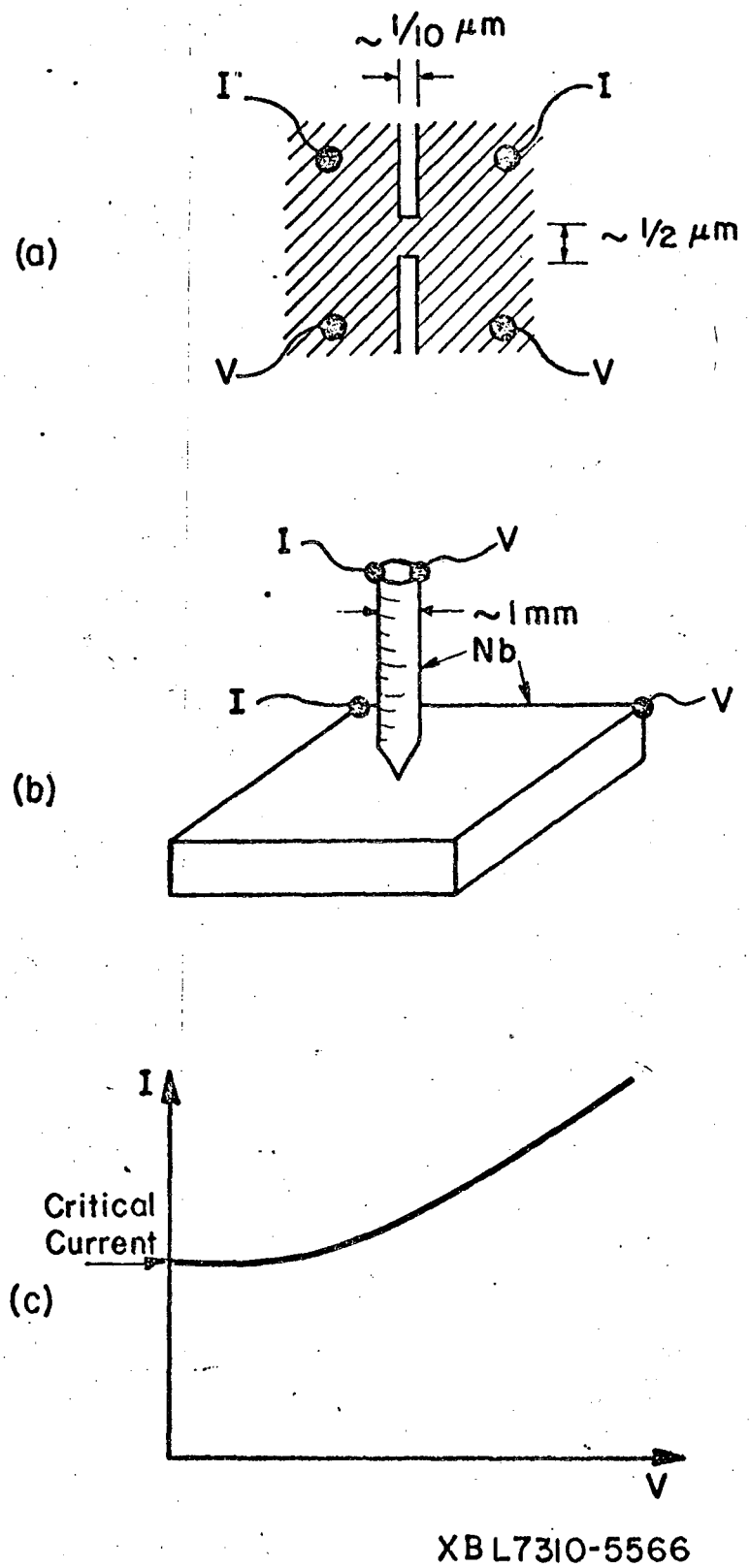
~1/10 μm
I
I
~1/2 μm
(a)
V
V
I
V
~1mm
Nb
I
V
(b)
I
Critical
Current
(c)
V
XBL7310-5566

Fig. 2

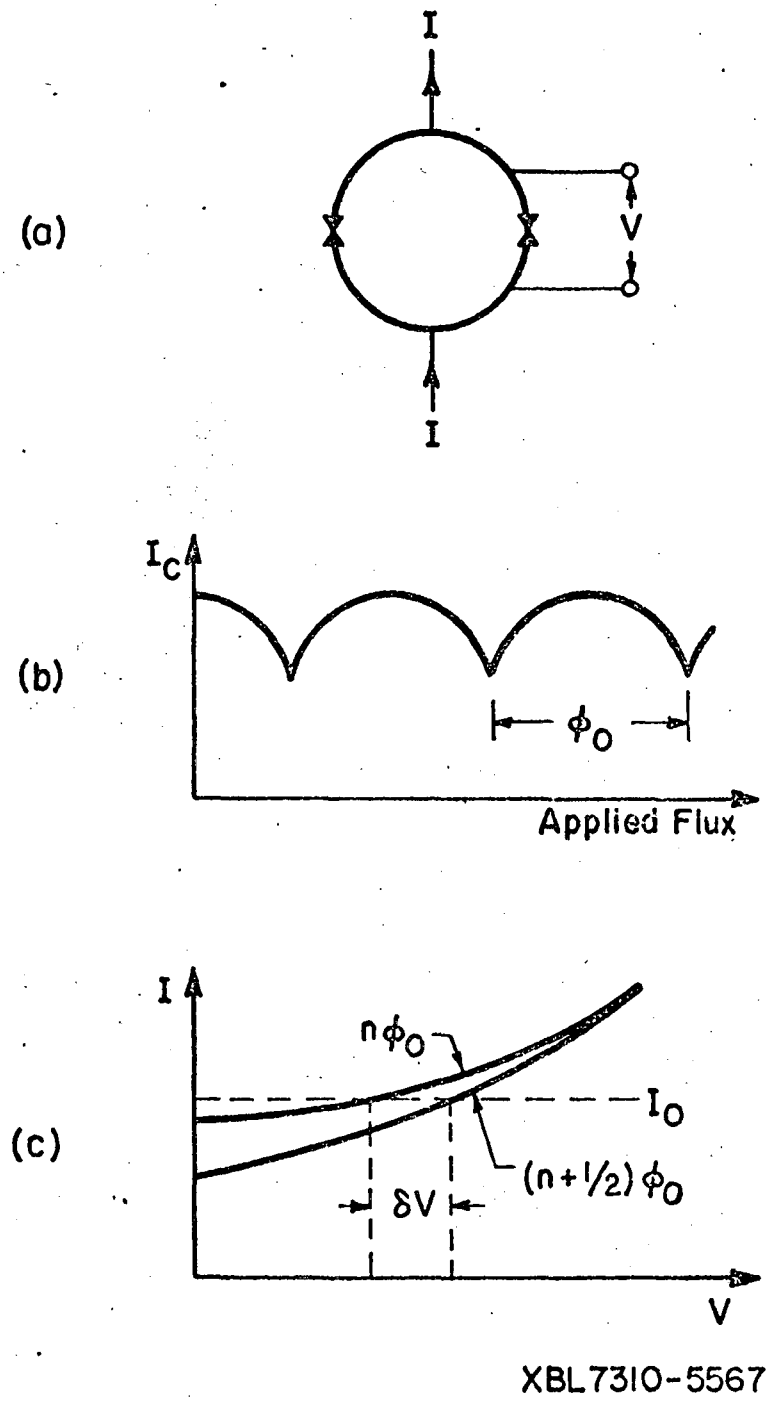
(a)
I
V
I
(b)
I_c
ϕ_0
Applied Flux
(c)
I
$n\phi_0$
I_0
$(n+1/2)\phi_0$
δV
V
XBL7310-5567

Fig. 3

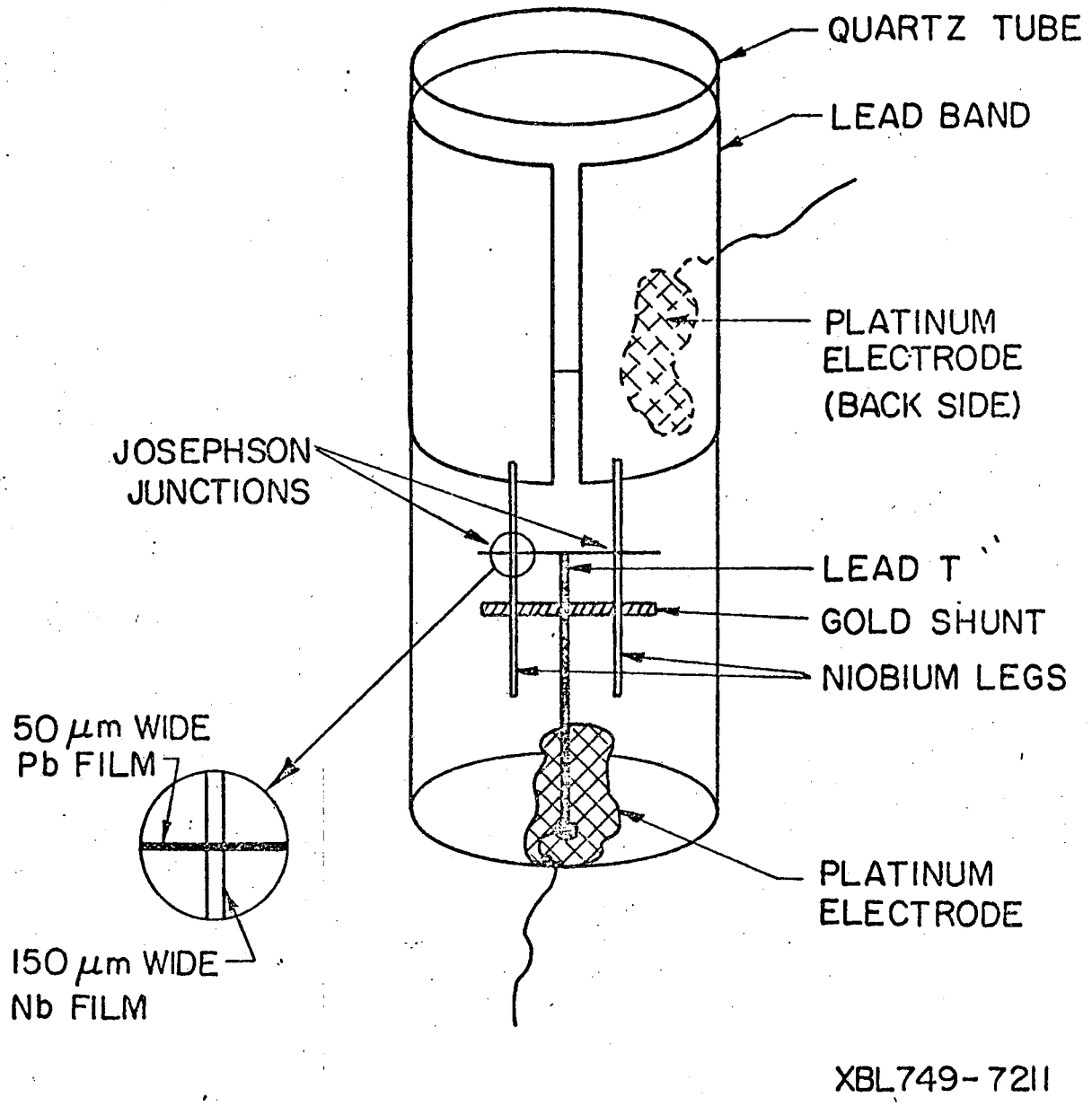
QUARTZ TUBE
LEAD BAND
PLATINUM ELECTRODE (BACK SIDE)
JOSEPHSON JUNCTIONS
LEAD T
GOLD SHUNT
NIOBIUM LEGS
50 μm WIDE Pb FILM
150 μm WIDE Nb FILM
PLATINUM ELECTRODE
XBL749-7211

Fig. 4

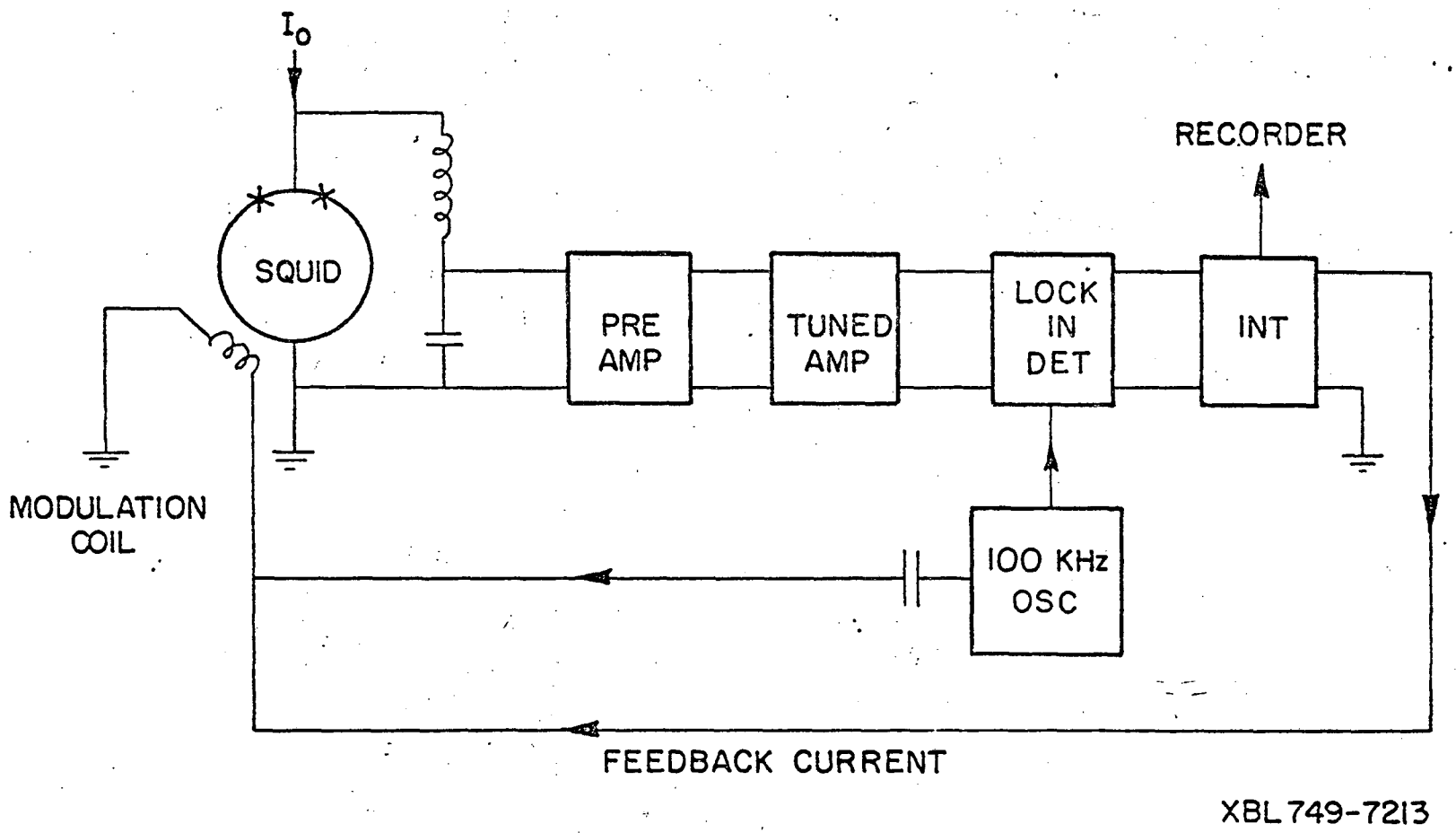
I_o
SQUID
MODULATION COIL
PRE AMP
TUNED AMP
LOCK IN DET
INT
RECORDER
100 KHz OSC
FEEDBACK CURRENT
XBL 749-7213

Fig. 5

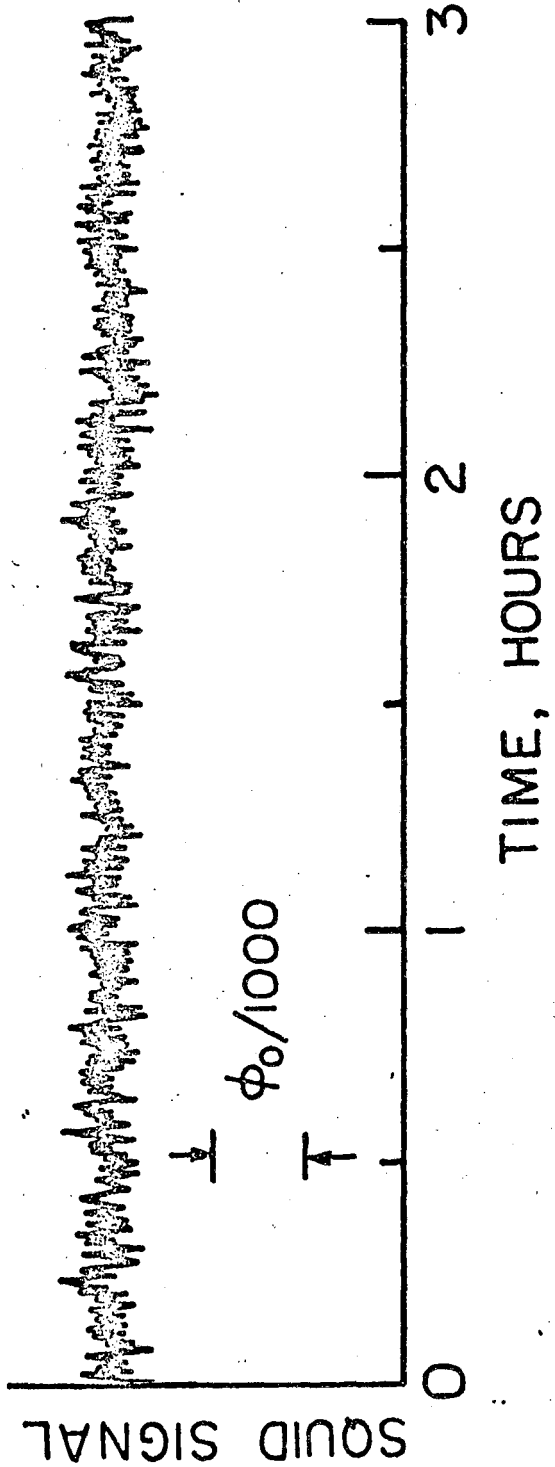

XBL749-7239A

Fig. 6

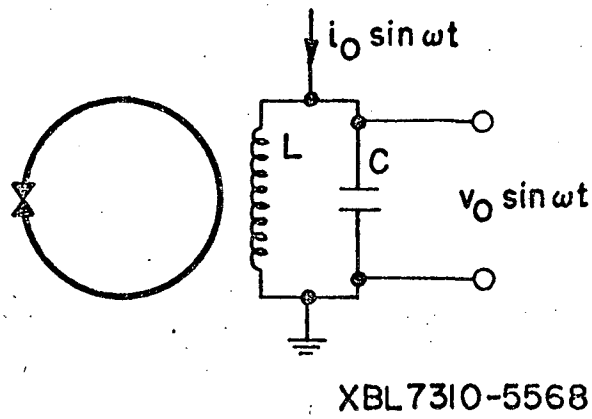

Fig. 7

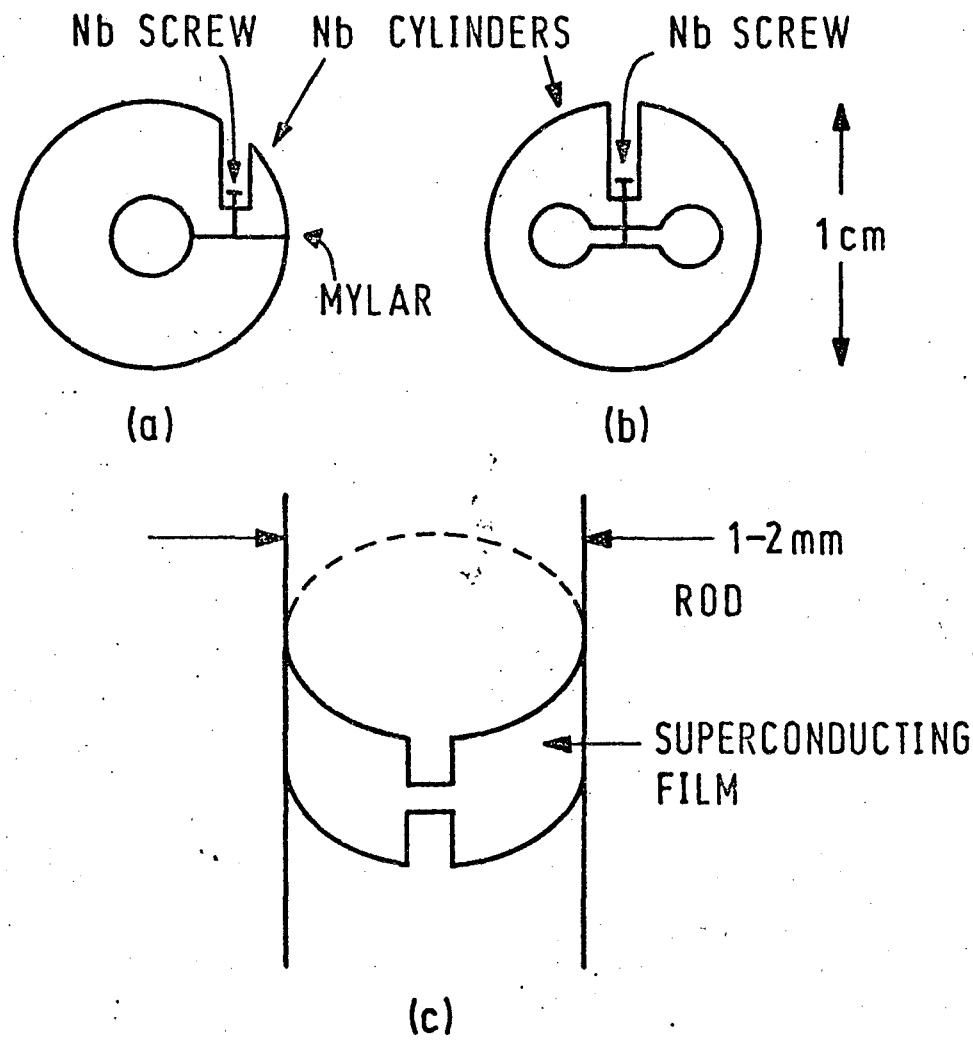

XBL 727-6617

Fig. 8

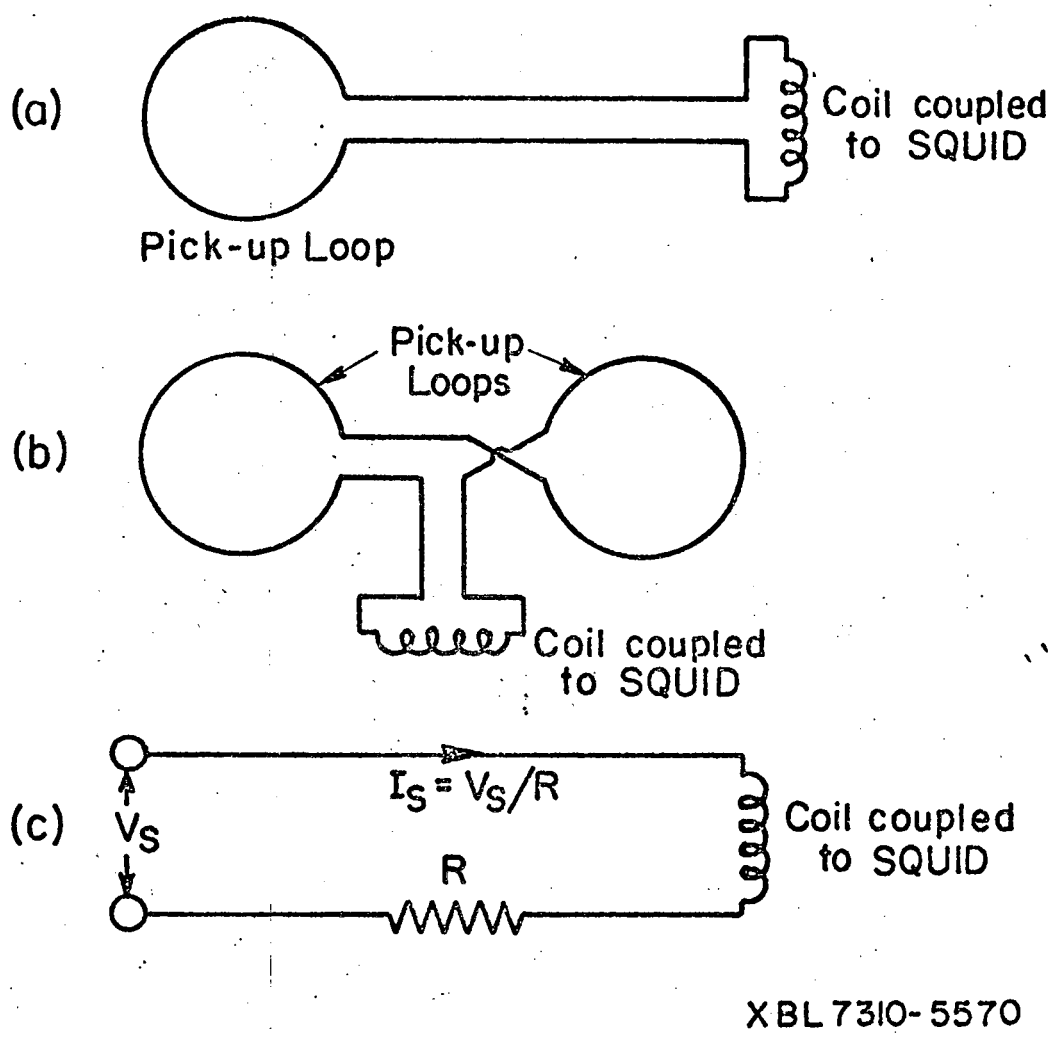
(a)
Coil coupled to SQUID
Pick-up Loop
(b)
Pick-up Loops
Coil coupled to SQUID
(c)
V_S
$I_S = V_S/R$
R
Coil coupled to SQUID
XBL 7310-5570

Fig. 9

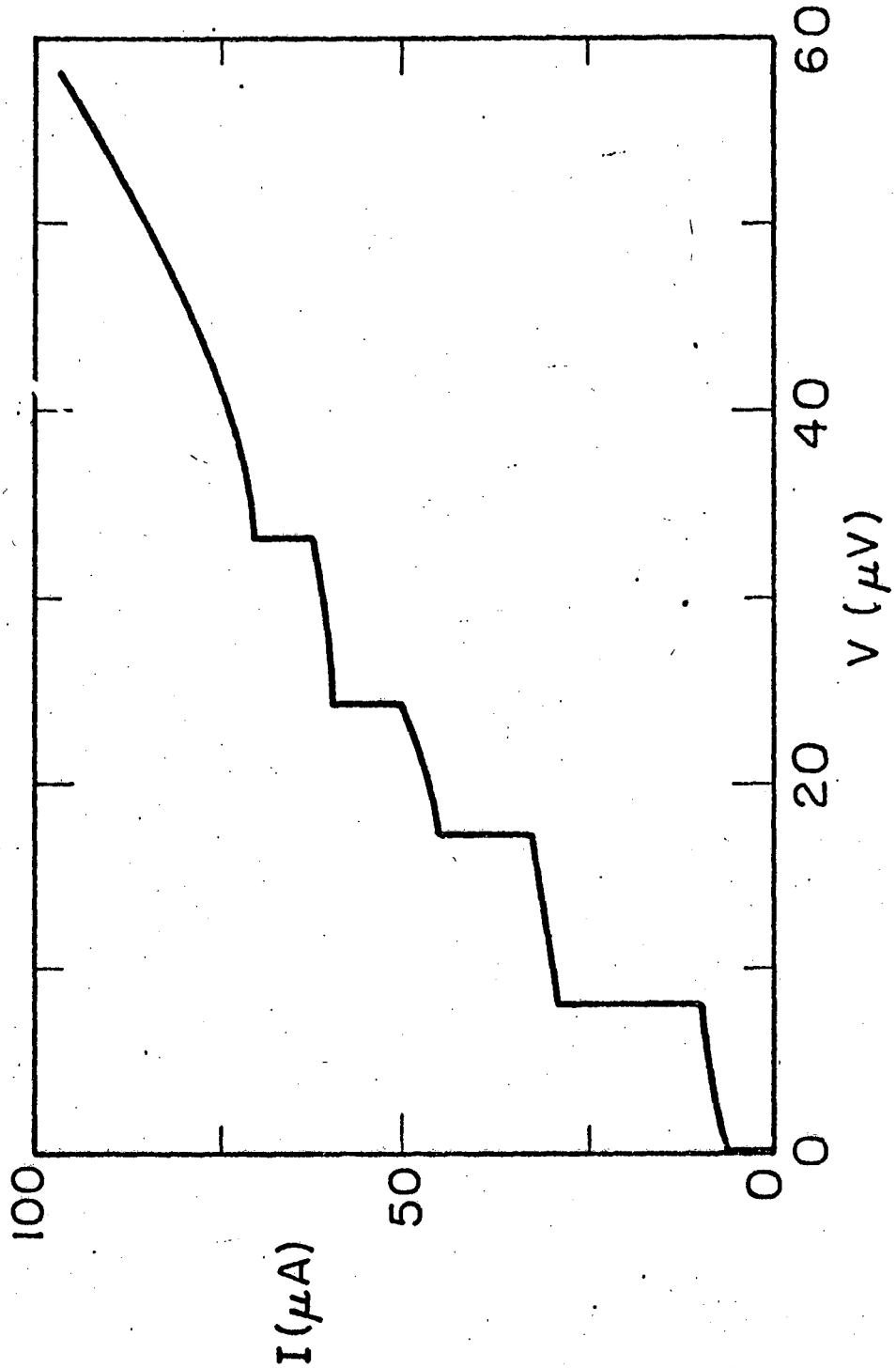

XBL 7310-5571

Fig. 10

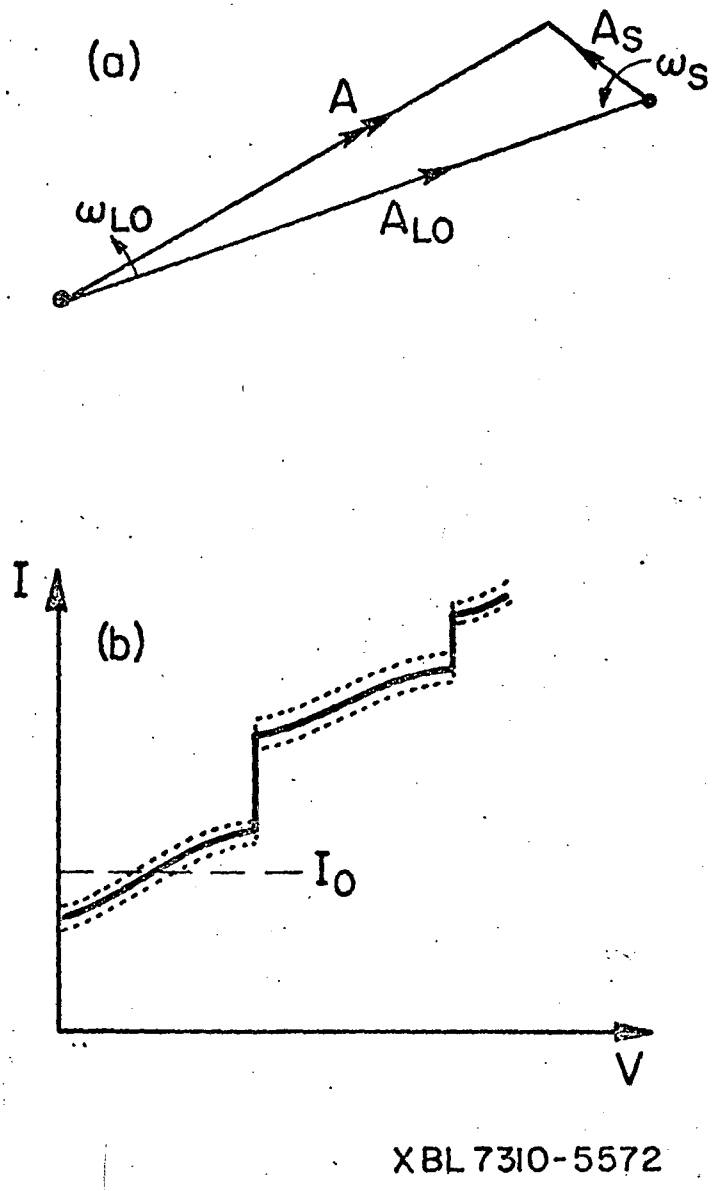

XBL 7310-5572

Fig. 11

0 0 0 0 4 2 0 7 0 0 8

LEGAL NOTICE

This report was prepared as an account of work sponsored by the United States Government. Neither the United States nor the United States Atomic Energy Commission, nor any of their employees, nor any of their contractors, subcontractors, or their employees, makes any warranty, express or implied, or assumes any legal liability or responsibility for the accuracy, completeness or usefulness of any information, apparatus, product or process disclosed, or represents that its use would not infringe privately owned rights.

TECHNICAL INFORMATION DIVISION
LAWRENCE BERKELEY LABORATORY
UNIVERSITY OF CALIFORNIA
BERKELEY, CALIFORNIA 94720